Drug Discovery I

Identification of Potent Ras Signaling Inhibitors by Pathway-Selective Phenotype-Based Screening**

*Oliver Müller, Eleni Gourzoulidou, Mercedes Carpintero, Ioanna-Maria Karaguni, Anette Langerak, Christian Herrmann, Tarik Möröy, Ludger Klein-Hitpaß, and Herbert Waldmann**

Phenotype-based screening of compound libraries utilizes chemistry and biology together at a very early phase of a chemical biological research program and identifies both potential biological targets and hit compounds in one step.[1] The power of the combination of this approach with modern chemistry and biology research techniques was recently demonstrated in the context of chemical genetics research.[2]

[*] Dipl.-Chem. E. Gourzoulidou, Dr. M. Carpintero, C. Herrmann, Prof. Dr. H. Waldmann
Max-Planck-Institut für molekulare Physiologie
Abteilung Chemische Biologie
Otto-Hahn-Strasse 11, 44227 Dortmund (Germany)
and
Universität Dortmund
Fachbereich 3, Organische Chemie
Fax: (+49) 231-133-2499
E-mail: herbert.waldmann@mpi-dortmund.mpg.de
Priv.-Doz. Dr. Dr. O. Müller, I.-M. Karaguni, A. Langerak
Max-Planck-Institut für molekulare Physiologie
Abteilung Strukturelle Biologie, Dortmund (Germany)
Prof. Dr. T. Möröy, Priv.-Doz. Dr. L. Klein-Hitpaß
Institut für Zellbiologie (Tumorforschung)
Universitätsklinikum Essen
Virchowstrasse 173, 45122 Essen (Germany)

[**] We thank Alfred Wittinghofer for his support. This study was supported by the Fonds der Chemischen Industrie and the European Union (Marie Curie Fellowship to M.C.).

Supporting information for this article is available on the WWW under http://www.angewandte.org or from the author.

  DOI: 10.1002/anie.200352587

The use of phenotypic change in entire organisms or unbiased cellular systems as a readout may render the identification of the biological target a complicated and laborious endeavor. The study of the reversal or change of the phenotype of a well-defined cellular system carrying known genomic lesions that directly correlate with a particular change in the microscopic phenotype should significantly improve the process of target identification. This improvement should be particularly evident if the genomic lesion affects a protein that acts at a prominent position of a multifaceted and branched signal transduction pathway. Pathway selectivity can be ensured by counterscreening two cell lines carrying lesions in different signaling pathways. In addition, an increase in efficiency can be expected if the compound class to be screened can be regarded as biologically prevalidated and if links from this compound class to the pathways of interest are known. The particular organism or cell type chosen should allow conclusive identification of the biological target while leaving room for identification of additional target proteins. Ideally, the biologically prevalidated compound classes should be based on "privileged structures," that is, structures that mediate binding to multiple biological targets.[3] If these prerequisites are fulfilled, one can expect that even a fairly small compound library will deliver hits with an appreciable rate.[4] Hits from such screens are expected to be of high quality because they have already been through a first round of biological validation. In addition, the library might yield hits for more than one target in a given pathway of interest, and possibly for targets in all pathways screened.

Herein we report the validation of this approach by employment of a phenotypic screen with a cell line activated in the Ras pathway for primary screening, and a cell line activated in the Wnt pathway for counterscreening (Figure 1).

The mutationally activated proto-oncoprotein Ras plays a significant role in the establishment of more than 30% of all human tumors. The development of small molecules that interfere with Ras signaling activity is a promising approach that is being pursued intensively in anticancer drug research.[5]

Antagonization of the interaction between Ras and its downstream effector Raf in the Ras signaling pathway poses a particularly challenging and difficult problem since this prototypical protein–protein interaction covers a large surface area.[5] Despite the attempts made in various intensive screening studies (including high-throughput screening approaches), inhibitors of the Ras–Raf interaction could only be identified in two cases.[6,7] In one of these cases, the metabolite **2** of the nonsteroidal antiinflammatory drug (NSAID) sulindac (**1**; see Table 1) was shown to be a Ras–Raf inhibitor. A compound derived from **1** was found to interfere with the Ras pathway as well, although its molecular target remained unidentified.[6]

Sulindac and its metabolites also influence various other biological phenomena, such as the inflammation-relevant cyclooxygenase pathway, an apoptosis-inducing pathway, and the tumor-relevant Wnt pathway (Figure 1).[8]

The established link between sulindac and the Ras pathway, and the ability of sulindac-derived compounds to interact with different proteins led us to synthesize a compound library with the underlying structure of this NSAID as a guiding scaffold. We analyzed the library for potential inhibitors of the Ras signal transduction pathway by using the phenotype-based strategy delineated above as the primary screen.

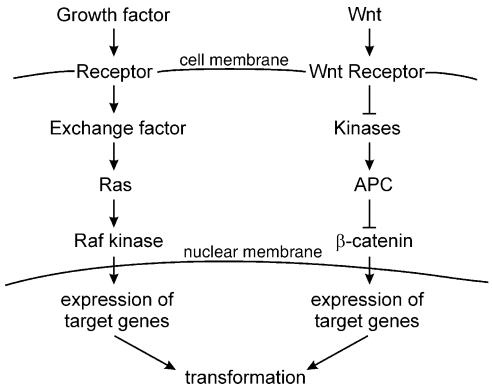

Figure 1. Schematic representation of the Ras (left) and the Wnt (right) pathways. Both pathways start outside the cell with the binding of a signaling protein to a transmembrane receptor. In the case of Ras, this binding leads, through a so-called exchange factor, to the activation of the Ras protein, which itself activates several kinases through the effector Raf kinase. The activation of the Wnt receptor leads to the activation, that is, the negative inhibition of the key signaling protein β-catenin through the action of several kinases and the tumor suppressor protein adenomatous polyposis coli (APC). The two pathways are formed by different proteins and are based in part on different biochemical principles. Nevertheless, both pathways lead to similar cellular effects: activation of target gene expression and transformation, that is, the transition from a normal cell into a tumor cell. By using suitable cell-culture models such as those used in the study described herein, cell transformation can be visualized by light microscopy.

The sulindac-derived compound library was synthesized on a solid support as shown in Scheme 1. Variously substituted indenylacetic acids **3**[9] were attached to 2-chlorotrityl chloride resin (obtained from Calbiochem–Novabiochem, loading 1.08 mmol g^{-1}, or from CBL–Patras, loading 1.6 mmol g^{-1}). Application of the Wang linker led to undesired cleavage of the indenylacetic acids under the basic conditions of the subsequent steps (see below). Resin-bound intermediates **4** were subjected to a Knoevenagel condensation with aromatic aldehydes to yield 188 sulindac analogues **5** in overall yields of 47–98% (calculated based on the initial loading of the resin) after release from the resin under acidic conditions. Critical to the successful execution of the Knoevenagel reaction is the choice of the base, which must be strong enough to mediate the condensation yet must not induce cleavage of the ester. Use of $(i\mathrm{Pr})_2\mathrm{NEt}$ or piperidine in DMF or toluene at up to 100 °C did not induce condensation. In the presence of sodium or potassium *tert*-butoxide the condensation proceeded, but the ester was also cleaved. DBU was used as the base of choice. In the presence of 10 equivalents DBU in DMF or toluene at 60 °C the desired products are formed without unwanted cleavage of the ester. The library was further expanded by subjecting immobilized indenylacetic acids **4** containing a bromine or an iodine atom in the aromatic ring to a Heck, Suzuki, or Sonogashira coupling, followed by the Knoevenagel condensation under

Table 1: Summary of the major results of the MTT assay and of analysis of cell biological parameters.[a] Data for sulindac (**1**) and its physiological sulfide metabolite **2** are shown for comparison.[6,12]

No.	Compound	Effects on MDCK-F3 cells	IC_{50} MDCK-F3 [μM]	IC_{50} ratio MDCK/MDCK-F3	IC_{50} ratio C57MG-Wnt-1/MDCK-F3
1	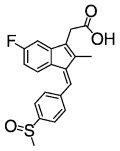	no effect	320	1/1	n.a.
2	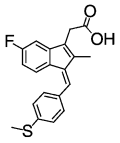	no effect	200	1/1	n.a.
5a	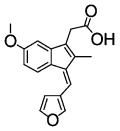	phenotype reversion, induction of apoptosis	50	10/1	6/1
5b	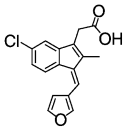	phenotype reversion, induction of apoptosis	90	3/1	2/1
5c	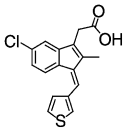	phenotype reversion	50	2/1	4/1
5d	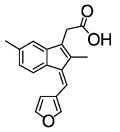	phenotype reversion, induction of apoptosis	50	4/1	6/1
5e	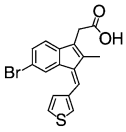	phenotype reversion	10	30/1	28/1
5f	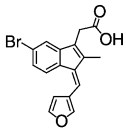	phenotype reversion, induction of apoptosis	40	2.5/1	6/1
5g	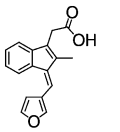	phenotype reversion, induction of apoptosis	50	3/1	6/1
5h	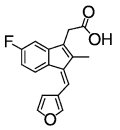	phenotype reversion	50	6/1	9/1

[a] Micromolar concentrations leading to a 50% decrease of the number of living cells are shown. The cell biological effects of 100 μM of each substance are shown. MTT = 3-(4,5-dimethylthiazol-2-yl)-2,5-diphenyltetrazolium bromide; n.a. = not applicable.

the conditions described above (Scheme 1). The conditions of the Pd-catalyzed reactions had to be optimized to obtain high yields. After substantial experimentation it was found that the

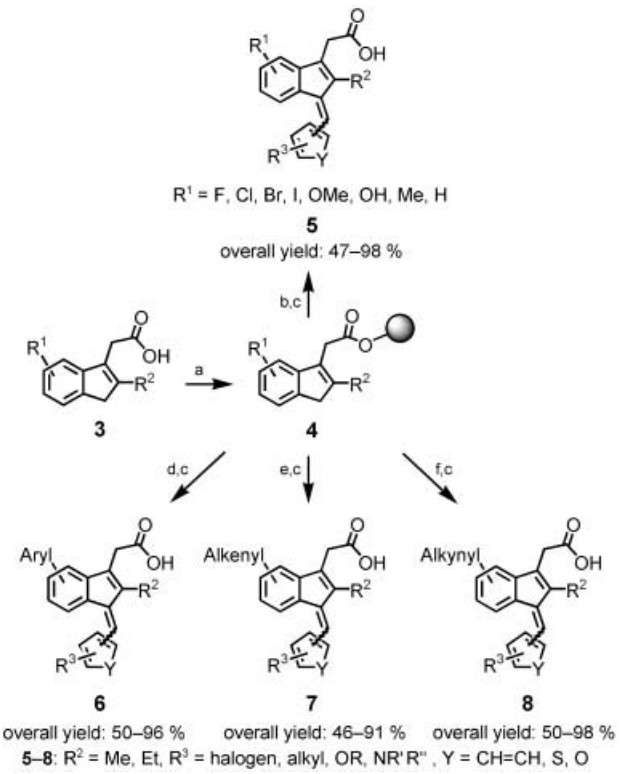

Scheme 1. a) 2-Chlorotrityl chloride resin, CH_2Cl_2, $(iPr)_2NEt$, 2 h, 21 °C; b) DBU, DMF or toluene, 60 °C, 16–48 h, aromatic aldehyde R^3CHO; c) 2% CF_3COOH in CH_2Cl_2; d) alkene (5 equiv), $[Pd_2(dba)_3]$ (0.5 equiv), P(*o*-tol)$_3$ (2 equiv), Et_3N/dioxane (1:1), Bu_4NBr (5 equiv), 85 °C, 20 h; e) boronic acid (10 equiv), $[Pd(PPh_3)_4]$ (0.35 equiv); $K_3PO_4 \cdot H_2O$ (20 equiv), DMF, 82 °C, 22 h; f) alkyne (20 equiv), CuI (0.3 equiv), DMF/Et_3N (1:1), PPh_3 (0.5 equiv), $[Pd(PPh_3)_4]$ (0.5 equiv), 85 °C, 20 h. DBU = 1,8-diazabicyclo[5.4.0]undec-7-ene, DMF = dimethylformamide; dba = *trans*,*trans*-dibenzylideneacetone.

Heck reaction proceeded best if $[Pd_2(dba)_3]$ was employed together with P(*o*-tol)$_3$ and nBu_4NBr as the catalyst system and the reaction was carried out in NEt_3/dioxane (1:1) at 85 °C. The Suzuki reaction proceeded efficiently at 82 °C in DMF in the presence of $[Pd(PPh_3)_4]$, and the Sonogashira reaction gave satisfactory results if $[Pd(PPh_3)_4]$ was used as the catalyst in DMF/NEt_3 (1:1) at 85 °C. It was necessary to use an alkene, alkyne, or boronic acid in 5–20-fold excess and to run the reactions for approximately 20 h to obtain acceptable results.

Knoevenagel condensation of the coupling products with different aromatic aldehydes followed by release from the solid support by treatment with acid led to sulindac analogues **6–8**, which have an aromatic substituent, an alkene or an alkyne, attached to the former indene benzene ring (Scheme 1). The desired sulindac analogues **6–8** were obtained in overall yields ranging from around 50% to over 90% by using these reaction sequences. The compounds had a purity in most cases of over 80% immediately after cleavage. Crude products with a purity of less than 80% were purified by flash chromatography on silica gel with ethyl acetate/cyclohexane (1:12 (v/v)) and 1% acetic acid as eluent to increase the purity to more than 80%. In total, 239 compounds were prepared.

NMR spectroscopic investigation with NOE techniques revealed that, in general, *Z* isomers were predominantly formed in the Knoevenagel reactions, with *Z*/*E* ratios of more than 9/1. The corresponding ethylene glycol esters of selected compounds were prepared (see the Supporting Information).

Phenotype-based screening of the library for in vivo effects was performed with the Madine–Darby canine kidney (MDCK) cell line for primary screening. MDCK cells are immortalized epithelial cells with a large and round phenotype. They grow in a monolayer, attached to each other by regular cell-to-cell contacts (Figure 2). MDCK cells can be

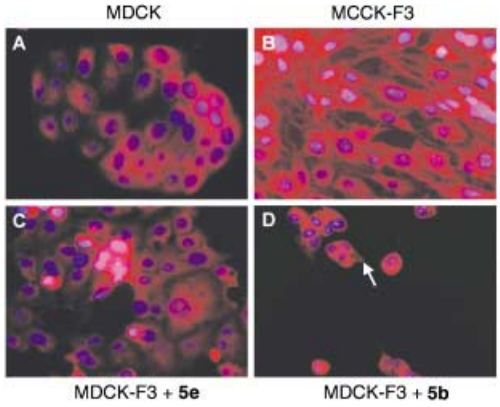

Figure 2. Representative results of the cell biological phenotype assays. Cellular morphology was visualized microscopically by immunostaining of intracellular F-actin fibers (red) and by staining nuclei with the DNA dye 4,6-diamidino-2-phenylindole (blue). A) MDCK cells have a round and regular phenotype. These cells grow attached to each other in epithelium-like, monolayer accumulations. B) MDCK-F3 cells show a spindle-shaped, longitudinal phenotype without regular cell contacts. C) MDCK-F3 cells treated with compound **5e** display a round morphology resembling that of the MDCK mother cells, but the treated cells form cell contacts. This change can be assigned to the reversion of the H-Ras-induced transformation. D) MDCK-F3 cells treated with compound **5b** show morphological signs of apoptosis, such as swollen, round cell bodies, condensed DNA, and apoptotic vesicles (arrow).

transformed by transfection with the H-Ras oncogene. The resulting F3 cells are long and spindlelike and grow in multiple layers without regular cell-to-cell contacts.[10] Since the H-Ras oncogene causes such a significant morphological alteration, cellular morphology can be used as a parameter for measuring the effects of a compound on the activated H-Ras pathway.[6] The specificity of the results obtained in the MDCK/MDCK-F3 assays was evaluated by counterscreening for the effects of all compounds on two cell lines. C57MG cells are murine epithelial mammary gland cells with a round and large phenotype. The transfection of C57MG cells with the Wnt-1 oncogene leads to similar morphological changes as the H-Ras transfection of MDCK cells described above: C57MG cells turn into spindle-shaped C57MG/Wnt-1 cells that grow without any contact inhibition.[11] Three parameters were investigated after incubation of cells with the compounds: In addition to detailed comparative analysis of the morphologies of treated and untreated cells, the influence of each compound on cell proliferation and cell survival was analyzed. These parameters were quantified by using a colorimetric proliferation assay with 3-(4,5-dimethylthiazol-2-yl)-2,5-diphenyltetrazolium bromide (MTT) as an indicator of the number of living cells.[12,13] Cells were also screened for signs of apoptosis. Swollen and vesicle-forming cell bodies and fragmented nuclei were taken as signs of apoptosis. To confirm the apoptotic effects of the compounds, cells were stained with annexin V, which binds to phosphatidylserine on the outer plasma membrane leaflet of cells in the early phases of apoptosis.[14,15]

In total, 189 compounds were subjected to the primary screen and analyzed for their ability to return the phenotype of MDCK-F3 cells to the phenotype of MDCK cells (Figure 2) and to induce apoptosis, as well as for their effect on the survival of Ras-transformed MDCK-F3 cells and C57MG/Wnt-1 cells in the MTT assay relative to the survival of the untransformed parent cell lines.

Compounds were scored as positive hits and selected for further analysis if they a) induced the reversion of the transformed phenotype of MDCK-F3 cells to the phenotype of MDCK cells or induced apoptosis, b) decreased the number of living cells by 50% at a concentration at least two–threefold lower when applied to MDCK-F3 cells than that required for MDCK cells, and c) showed at least two–threefold lower cytoxicity with both C57MG/Wnt-1 and C57MG cells than with MDCK and MDCK-F3 cells (Table 1; Figure 3).

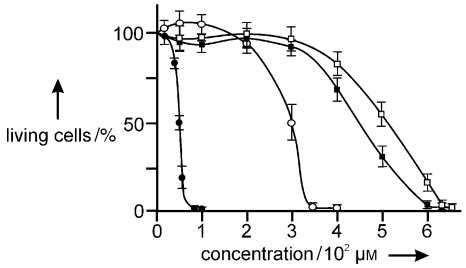

Figure 3. Representative cell survival and proliferation assay. The curves show the dependence of the percentage of living cells on the concentration of compound **5h**. H-Ras-transformed MDCK-F3 cells (filled circles) are more sensitive to compound **5h** than untransformed MDCK cells (open circles), which indicates that the compound affects the H-Ras pathway. C57MG-Wnt1 (filled squares) and C57MG cells (open squares), which were used for counterscreening in a control experiment, showed even lower sensitivity to **5h**.

Of all the tested compounds, 23 fulfilled the above criteria. The most promising compounds were **5a**–**5h** (see Table 1 and Figure 3). Closer inspection of the screening results reveals an initial structure–activity relationship for the compounds that fulfil the biological criteria. The most active compounds, **5a**–**5h**, carry a small substituent in the 5- or 6-position of the indenylacetic acid part of the molecule and a methyl group on the five-membered ring. The arylidene substituent should preferably be a five-membered electron-rich aromatic ring. Only carboxylic acids were active.

Taken together, the results demonstrate that phenotype-based pathway-selective screening provides new small-mole-

cule inhibitors of tumor-relevant pathways with high fidelity. Only a fairly small compound collection, one screen, and one counterscreen were employed in our investigation. The cell-biological screening and analysis of the sulindac-derived compound library yielded eight compounds with the desired profile. This result amounts to a hit rate of above 4%, a value that is entirely acceptable. The most active compound **5e** had an IC_{50} value of 10 μM in the cellular cytotoxicity assay and was 30 times more active than the parent molecule sulindac.

The results recorded for the phenotypic screen certainly reflect the fact that the underlying structure chosen for the compound library was based on that of sulindac, a compound whose influence on the Ras pathway had already been established and that can be regarded as biologically prevalidated. These results reinforce the notion forwarded above that biologically prevalidated compound classes should be used preferentially in chemical biology investigations in general, and in phenotype-based screens in particular, to obtain high hit rates.

In addition to high hit rates and hit compounds with significantly higher cellular activity than is often obtained with other methods, our results prove that phenotype screening based on a branched signaling pathway can deliver compounds that affect the pathway by acting on different targets. In the following paper,[16] we demonstrate that the majority of the compounds shown in Table 1 interfere with the Ras–Raf interaction. Such a screen may additionally yield compounds that target the pathway employed for counterscreening,[17] which renders the entire library synthesis, as well as the biological and biochemical investigations, very efficient.

Received: August 7, 2003 [Z52587]

Keywords: bioorganic chemistry · combinatorial chemistry · library screening · medicinal chemistry · signal transduction

[1] Review: B. R. Stockwell, *Neuron* **2002**, *36*, 559–562.
[2] See, for example, a) T. U. Mayer, T. M. Kapoor, S. J. Haggarty, R. W. King, S. L. Schreiber, T. J. Mitchison, *Science* **1999**, *286*, 971–974; b) S. Hotha, J. C. Yarrow, J. G. Yang, S. Garrett, K. V. Renduchintala, T. U. Mayer, T. M. Kappor, *Angew. Chem.* **2003**, *115*, 2481–2484; *Angew. Chem. Int. Ed.* **2003**, *42*, 2379–2382.
[3] B. E. Evans, K. E. Rittle, M. G. Bock, R. M. DiPardo, R. M. Freidinger, W. L. Whitter, G. F. Lundell, D. F. Veber, P. S. Anderson, R. S. L. Chang, V. J. Lorri, D. J. Cerino, T. B. Chen, P. J. Kling, K. A. Kunkel, J. P. Sprinter, J. Hirshfield, *J. Med. Chem.* **1988**, *31*, 2235–2246.
[4] R. Breinbauer, I. R. Vetter, H. Waldmann, *Angew. Chem.* **2002**, *114*, 3002–3015; *Angew. Chem. Int. Ed.* **2002**, *41*, 2879–2890.
[5] Reviews: a) H. Waldmann, A. Wittinghofer, *Angew. Chem.* **2000**, *112*, 4360–4383; *Angew. Chem. Int. Ed.* **2000**, *39*, 4192–4214; b) J. Downward, *Nat. Rev. Cancer* **2002**, *3*, 11–22.
[6] a) C. Herrmann, C. Block, C. Geisen, K. Haas, C. Weber, G. Winde, T. Moroy, O. Müller, *Oncogene* **1998**, *17*, 1769–1776; b) I. M. Karaguni, P. Herter, P. Debruyne, S. Chtarbova, A. Kasprzynski, U. Herbrand, M. R. Ahmadian, K. H. Glusenkamp, G. Winde, M. Mareel, *Cancer Res.* **2002**, *62*, 1718–1723.
[7] J. Kato-Stankiewicz, I. Hakimi, G. Zhi, J. Zhang, I. Serebriiskii, L. Guo, H. Edamatsu, H. Koide, S. Menon, R. Eckl, S. Sakamuri, Y. Lu, Q.-Z. Chen, S. Agarwal, W. R. Baumbach, E. A. Golemis, F. Tamanoi, V. Khazak, *Proc. Natl. Acad. Sci. USA* **2002**, *99*, 14398–14403.
[8] a) M. J. Thun, S. J. Henley, C. Patrono, *J. Natl. Cancer Inst.* **2002**, *94*, 252–266; b) E. T. Goluboff, *Expert Opin. Invest. Drugs* **2001**, *10*, 1875–1882; c) I.-M. Karaguni, M. Carpintero, E. Gourzoulidou, L. Klein-Hitpaß, T. Möröy, H. Waldmann, O. Müller, unpublished work.
[9] a) T.-Y. Shen, B. E. Witzel, H. Jones, B. O. Linn, R. B. Greenwald (Merck and Co.), DE 2039426, **1971** [*Chem. Abstr.* **1971**, *74*, 141379]; b) A. Bhattacharya, B. Segmuller, A. Ybarra, *Synth. Commun.* **1996**, *26*, 1775–1784.
[10] J. Behrens, M. M. Mareel, F. M. Van Roy, W. Birchmeier, *J. Cell Biol.* **1989**, *108*, 2435–2447.
[11] H. Shimizu, M. A. Julius, M. Giarre, Z. Zheng, A. M. Brown, J. Kitajewski, *Cell Growth Differ.* **1997**, *8*, 1349–1358.
[12] I. M. Karaguni, K. H. Glusenkamp, A. Langerak, C. Geisen, V. Ullrich, G. Winde, T. Möröy, O. Müller, *Bioorg. Med. Chem. Lett.* **2002**, *12*, 709–713.
[13] F. Denizot, R. Lang, *J. Immunol. Methods* **1986**, *89*, 271–277.
[14] S. J. Martin, C. P. Reutelingsperger, A. J. McGahon, J. A. Rader, R. C. van Schie, D. M. LaFace, D. R. Green, *J. Exp. Med.* **1995**, *182*, 1545–1556.
[15] M. van Engeland, L. J. Nieland, F. C. Ramaekers, B. Schutte, C. P. Reutelingsperger, *Cytometry* **1998**, *31*, 1–9.
[16] H. Waldmann, I. M. Karaguni, M. Carpintero, E. Gourzoulidou, C. Herrmann, C. Brockmann, H. Oschkinat, O. Müller, *Angew. Chem.* **2004**, *116*, 460; *Angew. Chem. Int. Ed.* **2004**, *43*, 454 (following article in this issue).
[17] H. Waldmann, O. Müller, unpublished results.

